



Lifetime of the Bose Gas with Resonant Interactions

B. S. Rem, A. T. Grier, I. Ferrier-Barbut, U. Eismann, T. Langen, N. Navon, L. Khaykovich, Felix Werner, Dmitry Petrov, F. Chevy, et al.

► To cite this version:

B. S. Rem, A. T. Grier, I. Ferrier-Barbut, U. Eismann, T. Langen, et al.. Lifetime of the Bose Gas with Resonant Interactions. 2012. <hal-00768038>

HAL Id: hal-00768038

<https://hal.science/hal-00768038v1>

Preprint submitted on 20 Dec 2012

HAL is a multi-disciplinary open access archive for the deposit and dissemination of scientific research documents, whether they are published or not. The documents may come from teaching and research institutions in France or abroad, or from public or private research centers.

L'archive ouverte pluridisciplinaire **HAL**, est destinée au dépôt et à la diffusion de documents scientifiques de niveau recherche, publiés ou non, émanant des établissements d'enseignement et de recherche français ou étrangers, des laboratoires publics ou privés.



HAL Authorization

Lifetime of the Bose Gas with Resonant Interactions

B. S. Rem,¹ A. T. Grier,¹ I. Ferrier-Barbut,¹ U. Eismann,¹ T. Langen,² N. Navon,¹
L. Khaykovich,^{1,3} F. Werner,¹ D. S. Petrov,^{4,5} F. Chevy,¹ and C. Salomon¹

¹*Laboratoire Kastler-Brossel, École Normale Supérieure,
CNRS and UPMC, 24 rue Lhomond, 75005 Paris, France*

²*Vienna Center for Quantum Science & Technology,
Atominsitut, TU Wien, Stadionallee 2, 1020 Wien, Austria*

³*Department of Physics, Bar-Ilan University, Ramat-Gan, 52900 Israel*

⁴*Université Paris-Sud, CNRS, LPTMS, UMR8626, Orsay, F-91405, France*

⁵*Russian Research Center Kurchatov Institute, Kurchatov Square, 123182 Moscow, Russia*

(Dated: December 20, 2012)

We study the lifetime of a Bose gas at and around unitarity using a Feshbach resonance in lithium 7. At unitarity, we measure the temperature dependence of the three-body decay coefficient L_3 . Our data follow a $L_3 = \lambda_3/T^2$ law with $\lambda_3 = 2.5(3)_{\text{stat}}(6)_{\text{sys}} \times 10^{-20} (\mu\text{K})^2 \text{cm}^6 \text{s}^{-1}$ and are in good agreement with our analytical result based on the zero-range theory. Varying the scattering length a at fixed temperature, we investigate the crossover between the finite-temperature unitary region and the previously studied regime where $|a|$ is smaller than the thermal wavelength. We find that L_3 is continuous across resonance, and over the whole $a < 0$ range our data quantitatively agree with our calculation.

PACS numbers: 03.75.Ss, 05.30.Fk, 32.80.Pj, 34.50.-s

Recent advances in manipulating cold atomic vapors have enabled the study of Fermi gases at the unitary limit where the scattering length a describing two-body interactions becomes infinite. It has been demonstrated both experimentally and theoretically that in this limit the system is characterized by a scale invariance leading to remarkably simple scaling laws [1]. By contrast, most experimental results on Bose-Einstein condensates were obtained in the weakly interacting regime. Recent experimental results on bosons near Feshbach resonances have revived the interest in strongly interacting bosons [2]: the development of experimental tools has enabled a precise test of the Lee-Huang-Yang corrections [3, 4], and several theoretical papers have studied the hypothetical unitary Bose gas at zero [5–8] or finite [9] temperature.

Experimental investigation of ultracold bosons near unitarity has been hampered by the fast increase of the three-body recombination rate close to a Feshbach resonance [10, 11]. In this case, the number of trapped atoms $N(t)$ follows the usual three-body law

$$\dot{N} = -L_3 \langle n^2 \rangle N, \quad (1)$$

where $\langle n^2 \rangle = \int d^3r n^3(\mathbf{r})/N$ is the mean square density and L_3 is the three-body loss rate constant. In the zero-temperature limit L_3 increases as $\hbar a^4/m$ [12] multiplied by a dimensionless log-periodic function of a revealing Efimov physics [15–24]. At finite temperature, L_3 saturates when a becomes comparable to the thermal wavelength $\lambda_{\text{th}} = h/\sqrt{2\pi m k_B T}$, and $L_3 \sim \hbar a^4/m \sim \hbar^5/m^3 (k_B T)^2$ [9, 25, 27]. This saturation suggests that a non-quantum-degenerate Bose gas near a Feshbach resonance will maintain quasi-thermal equilibrium [9]. Indeed, in this regime, $|a| \gtrsim \lambda_{\text{th}}$ and $n\lambda_{\text{th}}^3 \ll 1$. Thus, the elastic collision rate

$\gamma_2 \propto \hbar \lambda_{\text{th}} n/m$ is much higher than the three-body loss rate $\gamma_3 = L_3 n^2 \propto \hbar \lambda_{\text{th}}^4 n^2/m$. Experimental and numerical evidence for a saturation of L_3 were reported in [3, 20, 25]. A theoretical upper bound compatible with this scaling was derived in [26] assuming that only the lowest 3-body hyperspherical harmonic contributes, an assumption which breaks down when $|a|$ exceeds λ_{th} .

In this Letter, we measure the temperature dependence of the unitary three-body recombination rate and find agreement with a $L_3 \propto 1/T^2$ scaling law. In a second set of measurements performed at constant temperature we study L_3 versus a . We show how this function smoothly connects to the zero-temperature calculations when $|a| \ll \lambda_{\text{th}}$. These observations are explained by a general theoretical result for $L_3(a, T)$, exact in the zero-range approximation, that we derive in the second part. Our theory allows for a complete analytic description of the unitary case and, in particular, predicts (weak) log-periodic oscillations of the quantity $L_3 T^2$. Our findings quantify the ratio of good-to-bad collisions in the system and provide a solid ground for future studies of strongly interacting Bose gases. Furthermore, on the $a < 0$ side, experiments have so far detected a single Efimov trimer [3, 21–23, 30]. Our analysis predicts that a second Efimov trimer of very large size should be detectable in ^7Li at temperatures on the order of a few microkelvins.

Our experimental setup was presented in [28]. After magneto-optical trapping and evaporation in a Ioffe magnetic trap down to $\simeq 30 \mu\text{K}$, $\simeq 2 \times 10^6$ ^7Li atoms are transferred into a hybrid magnetic and dipole trap in the state $|1, 1\rangle$. The transverse confinement is obtained by a single laser beam of waist $43(1) \mu\text{m}$ and wavelength 1073 nm , while the longitudinal trapping is enhanced

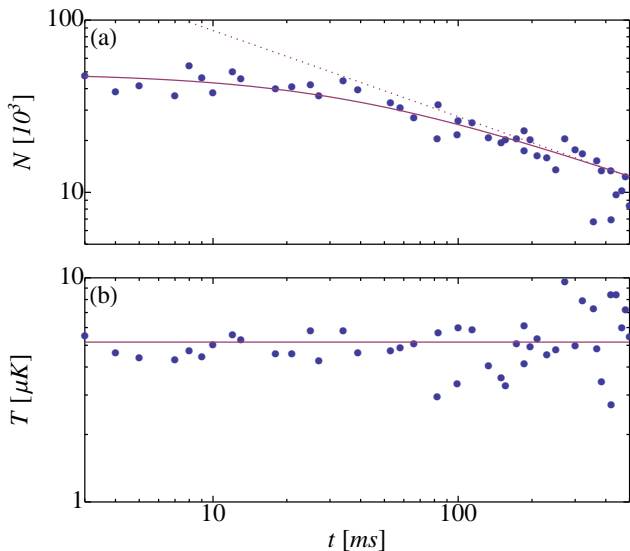


FIG. 1: Time dependence of the atom number (a) and temperature (b) for $U = \eta k_B T$, with $T = 5.2(4) \mu\text{K}$, $\eta = 7.4$ and (uncorrected) $L_3 = 1.2(2)_{\text{stat}} \times 10^{-21} \text{cm}^6 \text{s}^{-1}$. The dotted line shows the long time $t^{-1/2}$ dependence of the number of atoms.

by a magnetic curvature. The resulting potential has a cylindrical symmetry around the propagation axis of the laser and is characterized by trapping frequencies $0.87 \text{ kHz} < \omega_\rho/2\pi < 3.07 \text{ kHz}$ and $18 \text{ Hz} < \omega_z/2\pi < 49 \text{ Hz}$. Further cooling is achieved by applying a homogeneous magnetic field $B \simeq 718 \text{ G}$ for which the scattering length is $\simeq 200a_0$, and decreasing the depth of the trapping potential down to a variable value U' allowing us to vary the final temperature of the cloud. Afterwards, the dipole trap is recompressed to a value $U > U'$, to prevent significant atom loss due to the enhanced evaporation rate, see below. At each T we choose U so as to maintain the temperature constant during the three-body loss rate measurement. Finally, the magnetic field is ramped in 100–500 ms to $B_0 \simeq 737.8(3) \text{ G}$ where the scattering length a diverges [4]. We then measure the total atom number N remaining after a variable waiting time t and the corresponding T , using *in situ* imaging of the thermal gas.

Our data are limited to the range of temperature $1 \mu\text{K} \leq T \leq 10 \mu\text{K}$. For $T \gtrsim 1 \mu\text{K}$, the rate $\gamma_3 = -\dot{N}/N$ remains small with respect to other characteristic rates in our cloud (elastic scattering rate, trapping frequencies), which guarantees that a quasi-thermal equilibrium is maintained. We check that for these parameters the *in situ* integrated density profile is indeed gaussian, and we use it to extract the temperature of the cloud, found to be in agreement with that of time of flight. The peak phase-space density varies within $0.07 \times 10^{-2} < n_0 \lambda_{\text{th}}^3 < 1.1 \times 10^{-2}$. A

typical time dependence of N and T is shown in Fig. 1. The time dependence of the atom number is fitted using the usual three-body recombination law Eq. (1) [35]. For a non-degenerate gas of temperature T , the density profile is gaussian, and we have $\langle n^2 \rangle = N^2 A(T) = N^2 (m \bar{\omega}^2 / 2\pi \sqrt{3} k_B T)^3$, with $\bar{\omega} = (\omega_\rho^2 \omega_z)^{1/3}$ being the mean trapping frequency. We then have:

$$\dot{N} = -L_3(T) A(T) N^3. \quad (2)$$

Assuming constant temperature, integrating Eq. (2) gives

$$N(t) = \frac{N(0)}{\sqrt{1 + 2A(T)L_3(T)N^2(0)t}}, \quad (3)$$

which we use as a fitting function to analyze $N(t)$, and extract $L_3(T)$ as shown in Fig. 1.

Because of their n^3/T^2 dependence, three-body losses preferentially remove atoms of low kinetic energy and those located at the center of the trap where the density is the highest and potential energy is the smallest. As a result, three-body loss events heat up the cloud [12]. We ensure constant temperature by operating with a typical trap depth $U \simeq \eta k_B T$ with $6 \leq \eta \leq 8$, for which the residual evaporation then balances recombination heating, see Fig. 1b. This ensures that L_3 is time independent, but, as a drawback, evaporation contributes to losses. To quantify the relative importance of evaporative and three-body losses, we first note that an atom expelled by evaporation removes on average an energy $\simeq (\eta + \kappa) k_B T$, where, following [13], we take κ from [14], while each three-body event leaves on average an excess heat of $\delta k_B T$ per particle. Extending the derivation of [12] to the case of an energy dependent three-body loss rate $\propto E^{-2}$, we obtain $\delta = 5/3$ [36]. The energy balance required to keep the temperature constant thus implies that the evaporation rate is $\simeq \delta/(\eta + \kappa - 3)$ times smaller than the three-body loss rate. Neglecting this effect would induce a systematic overestimation of L_3 of about 50 % for $\eta = 6$ and 30 % for $\eta = 8$. Therefore, we apply this systematic correction to our data.

The temperature dependence of L_3 obtained from our measurements at unitarity is shown in Fig. 2. It is well fit by the scaling law $L_3(T) = \lambda_3/T^2$, with $\lambda_3 = 2.5(3)_{\text{stat}} \times 10^{-20} (\mu\text{K})^2 \text{cm}^6 \text{s}^{-1}$ as the best-fit value. In order to discuss the systematic uncertainty of this measurement we note that the quantity $L_3 T^2$ scales in all experimental parameters identically to the thermodynamic quantity $(\mu^2/P)^2$ of a zero-temperature BEC, with chemical potential μ , and pressure P [36]. We use this relation to calibrate our experimental parameters [4] and obtain a systematic uncertainty on λ_3 of $\leq 25\%$ resulting in $\lambda_3 = 2.5(3)_{\text{stat}}(6)_{\text{sys}} \times 10^{-20} (\mu\text{K})^2 \text{cm}^6 \text{s}^{-1}$.

We now study the a -dependence of L_3 on both sides of the resonance by employing the same experimental procedure as in the unitary case. We tune the scattering length

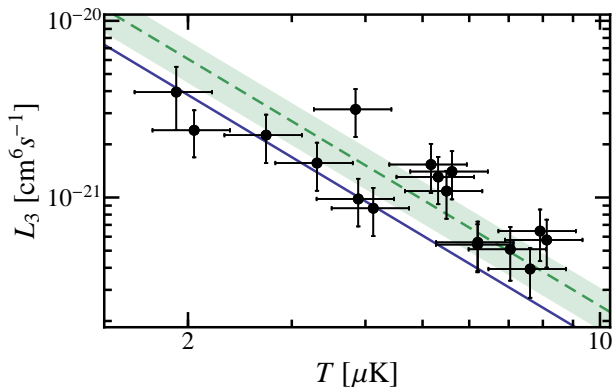


FIG. 2: Temperature dependence of the three-body loss rate L_3 . Filled circles: experimental data; green dashed line: best fit to the data $L_3(T) = \lambda_3/T^2$ with $\lambda_3 = 2.5(3)_{\text{stat}}(6)_{\text{sys}} \times 10^{-20} (\mu\text{K})^2 \text{cm}^6 \text{s}^{-1}$; the green band shows the 1σ quadrature sum of uncertainties. Solid line: prediction from Eq. (5), $\lambda_3 = 1.52 \times 10^{-20} (\mu\text{K})^2 \text{cm}^6 \text{s}^{-1}$ with $\eta_* = 0.21$ from [29, 30].

while keeping the temperature within 10% of 5.9 μK , see Fig. 3. The excess heat δ entering in the correction now depends on the value of ka . The correction is applied to all data points (filled circles) except in the range $1500 a_0 < a < 5000 a_0$ (open circles), where the assumptions of our model are not applicable [36]. In the limit $|a| \gg \lambda_{\text{th}}$, we observe that $L_3(a)$ saturates to the same value on both sides of the resonance. In the opposite limit $|a| \ll \lambda_{\text{th}}$, our data connect to the zero temperature behavior [18] studied experimentally in [20–24]. On the $a < 0$ side, the dashed line is the zero-temperature prediction for L_3 from [18]. We clearly see that finite temperature reduces the three-body loss rate. On the $a > 0$ side, temperature effects become negligible for $a < 2000 a_0$ as testified by our measurements performed on a low temperature Bose-Einstein condensate (green squares) which agree with the total recombination rate to shallow and deep dimers calculated at $T = 0$ in [18] (dashed line). The data around unitarity and on the $a < 0$ side are seen to be in excellent agreement with our theory Eq. (4) described below.

In order to understand the dependence $L_3(a, T)$ theoretically, we employ the S -matrix formalism developed in [18, 31, 32]. According to the method, at hyper-radii $R \gg |a|$ one defines three-atom scattering channels ($i = 3, 4, \dots$) for which the wavefunction factorizes into a normalized hyperangular part, $\Phi_i(\hat{R})$, and a linear superposition of the incoming, $R^{-5/2}e^{-ikR}$, and outgoing, $R^{-5/2}e^{+ikR}$, hyperradial waves. The channel $i = 2$ is defined for $a > 0$ and describes the motion of an atom relative to a shallow dimer. The recombination or relaxation to deep molecular states (with a size of order the van der Waals range R_e) requires inclusion of other atom-dimer channels. In the zero-range approximation,

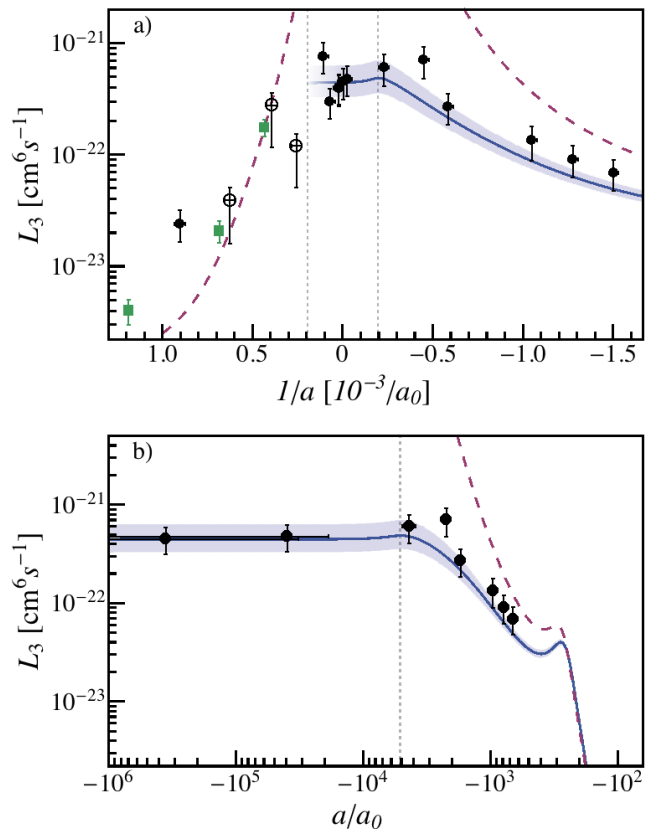


FIG. 3: a) Scattering-length dependence of the three-body rate constant $L_3(a)$ for constant $T = 5.9(6) \mu\text{K}$ (filled and open circles). For small positive a , $L_3(a)$ for a low temperature condensate is also shown (green squares). The solid blue line corresponds to our theoretical prediction Eq. (4) for $T = 5.9 \mu\text{K}$. The blue range is the same theory for 5.3 to 6.5 μK . The dashed lines represent the zero-temperature prediction for $L_3(a)$ [18]. All theory curves are for the ^7Li parameters $\eta_* = 0.21$ and $R_0 = 270 a_0$ measured in [29, 30]. The vertical dotted lines correspond to $|a|/\lambda_{\text{th}} = 1$. The open circles in the range $1500 a_0 < a < 5000 a_0$ are not corrected for residual evaporation as our model is not applicable. b) Logarithmic plot of the $a < 0$ side, displaying the two Efimov loss resonances.

valid when $R_e \ll R_m \equiv \text{Min}(1/k, |a|)$, the overall effect of these channels and all short-range physics in general can be taken into account by introducing a single Efimov channel ($i = 1$) defined for $R_e \ll R \ll R_m$: the wavefunction at these distances is a linear superposition of the incoming, $\Phi_1(\hat{R})R^{-2+is_0}$, and outgoing, $\Phi_1(\hat{R})R^{-2-is_0}$, Efimov radial waves. Here $s_0 \approx 1.00624$. The notion “incoming” or “outgoing” is defined with respect to the long-distance region $R_m \lesssim R \lesssim |a|$, so that, for example, the incoming Efimov wave actually propagates towards larger R whereas incoming waves in all other channels propagate towards smaller hyperradii. The matrix s_{ij} relates the incoming amplitude in the i^{th} channel with the outgoing one in the j^{th} channel and de-

scribes the reflection, transmission, and mixing of channels in the *long-distance* region. This matrix is unitary and independent of the short-range physics. The short-range effects are taken into account by fixing the relative phase and amplitude of the incoming and outgoing Efimov waves $R^2\Psi \propto (R/R_0)^{is_0} - e^{2\eta_*}(R/R_0)^{-is_0}$, where R_0 is the three-body parameter and the short-range inelastic processes are parametrized by $\eta_* > 0$, which implies that the number of triples going towards the region of $R \sim R_e$ is by the factor $e^{4\eta_*}$ larger than the number of triples leaving this region [33]. Braaten *et al.* [32] have shown that for a given incoming channel $i \geq 2$ the probability of recombination to deeply bound states is $P_i = (1 - e^{-4\eta_*})|s_{i1}|^2 / |1 + (kR_0)^{-2is_0}e^{-2\eta_*}s_{i1}|^2$ [34]. For $a < 0$, by using the fact that s_{11} is unitary ($\sum_{i=1}^{\infty} |s_{1i}|^2 = 1$) and averaging over the Boltzmann distribution we then obtain the total loss rate constant

$$L_3 = \frac{72\sqrt{3}\pi^2\hbar(1-e^{-4\eta_*})}{mk_{\text{th}}^6} \int_0^{\infty} \frac{(1-|s_{11}|^2)e^{-k^2/k_{\text{th}}^2}kdk}{|1+(kR_0)^{-2is_0}e^{-2\eta_*}s_{11}|^2}, \quad (4)$$

where $k_{\text{th}} = \sqrt{mk_B T}/\hbar$.

Note that in deriving Eq. (4) we closely followed [32] where the scattering length was assumed to be finite. However, we easily generalize this derivation to the case $a = \infty$, in which the channels become decoupled at distances $R \gg 1/k$ and the *long-distance* region can now be defined by $R \sim 1/k$. A less trivial result of our analysis is that for any ka there exists a unitary transformation of the matrix s_{ij} which leaves the element s_{11} invariant, but all channels with $i > 3$ become decoupled from the Efimov channel [36]. This transformation constructs a new large- R channel characterized by a certain hyperangular wavefunction $\tilde{\Phi}_3(\hat{R})$. For negative or infinite a this is the only channel that can “talk” to the lossy short-distance Efimov channel via a unitary 2×2 matrix. Therefore, the three-body loss rate can not exceed the so-called maximum value $L_3^{\text{max}} = 36\sqrt{3}\pi^2\hbar^5(k_B T)^{-2}/m^3$ reached in the case when the outgoing flux in this newly constructed channel vanishes. Previous derivations of L_3^{max} [26] essentially implied that $\tilde{\Phi}_3(\hat{R})$ is the lowest *non-interacting* hyperspherical harmonics. This approximation can be made only for $k|a| \ll 1$. In general, $\tilde{\Phi}_3(\hat{R})$ is *not* an eigenstate of the angular momentum operator. In particular, at unitarity $\tilde{\Phi}_3(\hat{R}) = \Phi_1(\hat{R})$ [36].

The function $s_{11}(ka)$ is calculated in [36]. At unitarity it equals $s_{11}(\infty) = -e^{-\pi s_0}e^{2i[s_0 \ln 2 + \text{Arg} \Gamma(1+is_0)]}$ and from Eq. (4) one sees that $L_3 T^2$ should be a log-periodic function of T . However, due to the numerically small value of $|s_{11}| \approx 0.04$, in the case of three identical bosons the oscillations are very small and L_3 is well approximated by setting $s_{11} = 0$:

$$L_3 \approx \frac{\hbar^5}{m^3} 36\sqrt{3}\pi^2 \frac{1 - e^{-4\eta_*}}{(k_B T)^2}. \quad (5)$$

This explains the $L_3 \propto T^{-2}$ experimental observation seen

in Fig. 2 at unitarity. Taking $\eta_* = 0.21$, which is the average of two measurements made for our ^7Li Feshbach resonance in [29, 30], we get $L_3 = \lambda_3/T^2$ with $\lambda_3 = 1.52 \times 10^{-20}(\mu\text{K})^2\text{cm}^6\text{s}^{-1}$. This is 40 % below the experimentally determined value without any adjustable parameter and the agreement between theory and experiment is 1.4σ . We should point out that Eq. (4) can be easily generalized to the case of other three-body systems with smaller s_0 . Then, the terms neglected in Eq. (5) can become important. They also become important in our system of three identical bosons when departing from resonance in the direction of $a < 0$. Then $|s_{11}(ka)|$ monotonically increases as a function of $1/k|a|$ reaching 1 in the limit $ka \rightarrow 0^-$, the argument of s_{11} also being a monotonic function of $1/k|a|$ [36]. The solid blue line in Fig. 3 is the result obtained from Eq. (4) using the same η_* as above and $R_0 = 270a_0$ also taken from [29, 30]. The shaded blue area reflects our experimental range of temperatures. More or less visible maxima of L_3 appear when the denominator in the integrand of Eq. (4) reaches its minimum, *i.e.*, becomes resonant. The approximate condition for this is $\text{Arg } s_{11}(ka) = \pi + 2s_0 \ln kR_0$ and the features become increasingly more pronounced for larger $|s_{11}|$ and smaller η_* . Note that from the viewpoint of the visibility of the maxima, decreasing $|a|$ is equivalent to decreasing \sqrt{T} . Fig 3b shows the pronounced resonance at $a = a_- \approx -274a_0$ observed in [29, 30]. This resonance is associated with the passage of an Efimov trimer through the three-atom threshold. Another Efimov trimer, larger in size by a factor of $e^{\pi/s_0} = 22.7$, is expected to go through the threshold at around $a \approx -6350a_0$ leading to another zero energy resonance. As we deduce from Eq. (4) and show in Fig. 3 for $5.9\mu\text{K}$, the thermally averaged remnants of this predicted resonance lead to a maximum of L_3 at $a \approx -5100a_0$. As seen in Fig. 3b the agreement between theory and experiment is very good over the entire $a < 0$ range.

Because of the existence of a shallow dimer state, the case $a > 0$ becomes, in general, a complicated dynamical problem which should take into account the atom-dimer and dimer-dimer relaxation as well as various non-universal factors: the finite trap depth, chemical imbalance between trapped shallow dimers and free atoms, and deviations from thermal equilibrium, possibly dependent on the preparation sequence. These issues require an extensive discussion beyond the scope of this Letter. The situation obviously simplifies in the case of very small a when the system is purely atomic and the three-body recombination to deep and shallow molecules leads to an immediate loss of three atoms.

Discussing the opposite limit of large $a > 0$, we first note that dimers are well defined when their size $\sim a$ is smaller than $n^{-1/3}$, which we assume in the following (the limit $na^3 \gg 1$ is equivalent to the case $a = \infty$). In the regime $a \gg \lambda_{\text{th}}$ we find using the Skorniakov-Ter-Martirosian equation that $s_{12} \rightarrow 0$ for $ka \rightarrow \infty$, which im-

plies that the atom-dimer relaxation rate vanishes and that shallow dimers remain at chemical quasi-equilibrium with the decaying atomic ensemble [36]. Shallow dimer formation and breakup are then balanced, so that the atomic decay is just given by Eq. (1). The expression of L_3 for $a > 0$ was obtained in [32] and reduces to Eq. (4) for $s_{12} \rightarrow 0$. We conclude that the loss rate must be continuous across the resonance, in accordance with our experimental data. Therefore, in Fig. 3a the result of Eq. (4) is simply continued to positive a for $a \gg \lambda_{\text{th}}$.

In summary, we have systematically studied the dependence of the three-body loss rate on T and a in a Bose gas near unitarity. The T^{-2} temperature dependence seems to contradict the well-known Arrhenius law $L_3 \propto \exp(-\Delta E/k_B T)$ for a chemical reaction with activation energy ΔE . This paradox is resolved by noting that three-body recombination occurs through the $-1/R^2$ Efimov three-body potential that does not display any potential hill. Moreover, a quantum interference effect in Efimov three-body scattering leads to an enhanced decay rate at a negative a , suggesting the possibility to observe the signature of a second Efimov trimer of large size. Another future direction is to explore the approach to the quantum degenerate regime and test whether the virial expansion of the unitary Bose gas can be measured by using quasi-equilibrium thermodynamics [9].

We acknowledge fruitful discussions with G. Shlyapnikov and F. Ferlaino, and support from Région Île de France (IFRAF), EU (ERC advanced grant Ferlodim), Institut Universitaire de France, and the Russian Foundation for Fundamental Research. T.L. acknowledges support by the Austrian Science Fund (FWF) through the Doctoral Programme CoQuS (W1210).

-
- [1] *BCS-BEC crossover and the Unitary Fermi Gas: Lecture Notes in Physics*, Vol. 836, W. Zwerger, ed. (Springer, Berlin, 2011).
- [2] S. E. Pollack, D. Dries, M. Junker, Y. P. Chen, T. A. Corcovilos, and R. G. Hulet, Phys. Rev. Lett. **102**, 090402 (2009).
- [3] R. J. Wild, P. Makotyn, J. M. Pino, E. A. Cornell, and D. S. Jin, Phys. Rev. Lett. **108**, 145305 (2012).
- [4] N. Navon, S. Piatecki, K. Günter, B. Rem, T.-C. Nguyen, F. Chevy, W. Krauth, and C. Salomon, Phys. Rev. Lett. **107**, 135301 (2011).
- [5] S. Cowell, H. Heiselberg, I. E. Mazets, J. Morales, V. R. Pandharipande, and C. J. Pethick, Phys. Rev. Lett. **88**, 210403 (2002).
- [6] J.-L. Song and F. Zhou, Phys. Rev. Lett. **103**, 025302 (2009).
- [7] Yu-Li Lee and Yu-Wen Lee, Phys. Rev. A **81**, 063613 (2010).
- [8] D. Borzov, M. S. Mashayekhi, S. Zhang, J.-L. Song, and F. Zhou, Phys. Rev. A **85**, 023620 (2012).
- [9] W. Li and T.-L. Ho, Phys. Rev. Lett. **108**, 195301 (2012).
- [10] S. Inouye, M. R. Andrews, J. Stenger, H.-J. Miesner, D. M. Stamper-Kurn, and W. Ketterle, Nature **392**, 151 (1998).
- [11] J. L. Roberts, N. R. Claussen, S. L. Cornish, and C. E. Wieman, Phys. Rev. Lett. **85**, 728 (2000).
- [12] T. Weber, J. Herbig, M. Mark, H.-C. Nägerl, and R. Grimm, Phys. Rev. Lett. **91**, 123201 (2003).
- [13] L. Luo, B. Clancy, J. Joseph, J. Kinast, A. Turlapov, and J. E. Thomas, New J. Phys. **8**, 213 (2006).
- [14] O. Luiten, M. Reynolds, and J. T. M. Walraven, Phys. Rev. A, **53**(1), 381389 (1996).
- [15] E. Nielsen and J. H. Macek, Phys. Rev. Lett. **83**, 1566 (1999).
- [16] B. D. Esry, Chris H. Greene, and James P. Burke, Phys. Rev. Lett. **83**, 1751 (1999).
- [17] P. F. Bedaque, E. Braaten, and H.-W. Hammer, Phys. Rev. Lett. **85**, 908 (2000).
- [18] E. Braaten and H.-W. Hammer, Phys. Rep. **428**, 259 (2006).
- [19] D. S. Petrov, in *Many-Body Physics with Ultra-Cold Gases: Lecture Notes of the Les Houches Summer Schools*, Vol. 94, C. Salomon, G. V. Shlyapnikov, and L. F. Cugliandolo, eds. (Oxford University Press, Oxford, 2013), arXiv:1206.5752.
- [20] T. Kraemer, M. Mark, P. Waldburger, J. G. Danzl, C. Chin, B. Engeser, A. D. Lange, K. Pilch, A. Jaakkola, H. C. Nägerl, and R. Grimm, Nature **440**, 315 (2006).
- [21] M. Zaccanti, B. Deissler, C. D'Errico, M. Fattori, M. Jona-Lasinio, S. Müller, G. Roati, M. Iguscio, and G. Modugno, Nat. Phys. **5**, 586 (2009).
- [22] S. E. Pollack, D. Dries, and R. G. Hulet, Science **326**, 1683 (2009).
- [23] N. Gross, Z. Shotan, S. Kokkelmans, and L. Khaykovich, Phys. Rev. Lett. **103**, 163202 (2009).
- [24] Ferlaino, F., Zenesini, A., Berninger, M., Huang, B., Nägerl, H. C., Grimm, R. Few-Body Systems, 121 (2011).
- [25] J. P. D'Incao, H. Suno, and B. D. Esry, Phys. Rev. Lett. **93**, 123201 (2004).
- [26] N. P. Mehta, S. T. Rittenhouse, J. P. D'Incao, J. von Stecher, and C. H. Greene, Phys. Rev. Lett. **103**, 153201 (2009).
- [27] J. P. D'Incao, C. H. Greene, and B. D. Esry, J. Phys. B: At. Mol. Opt. Phys. **42**, 044016 (2009).
- [28] S. Nascimbène, PhD thesis, ENS, 2010.
- [29] N. Gross, Z. Shotan, O. Machtey, S. Kokkelmans, and L. Khaykovich, C. R. Physique **12**, 4 (2011).
- [30] N. Gross, Z. Shotan, S. Kokkelmans, and L. Khaykovich, Phys. Rev. Lett. **105**, 103203 (2010).
- [31] V. Efimov, Sov. J. Nucl. Phys. **29**, 546 (1979).
- [32] E. Braaten, H.-W. Hammer, D. Kang, and L. Platter, Phys. Rev. A **78** (2008).
- [33] E. Braaten, H.-W. Hammer, and M. Kusunoki, Phys. Rev. A **67**, 022505 (2003).
- [34] Our s_{11} differs by a phase factor from the one defined in [32], see [36].
- [35] We neglect four- and higher-body losses which, dimensionally, are expected to be suppressed by a factor $n_0 \lambda_{\text{th}}^3$ [26].
- [36] See Supplemental Material for more information on the calculation of s_{11} ; a discussion of s_{12} , atom-dimer relaxation, and chemical equilibrium in the limit $a \rightarrow \infty$; a construction of the unitary transformation for the matrix s_{ij} ; an interpretation of Eq. (4) in terms of a Fabry-Perot interferometer; and a discussion of evaporation and experimental uncertainties.